Pinning Centers in ISD-MgO Coated Conductors via EB-PVD

Benjamin H. Stafford, Max Sieger, Oleksiy Troshyn, Ruben Hühne, Jens Hänisch, Markus Bauer, Bernhard Holzapfel, and Ludwig Schultz

***Abstract*—$GdBa_2Cu_3O_{7-x}$ (GdBCO) films doped with up to 13.6 mol.% $BaHfO_3$ (BHO) have been grown by electron beam physical vapor deposition (EB-PVD). A critical current density J_c at 30 K, 3 T of 2.34 MA/cm^2 has been achieved for a doping level of 10.6 mol.%. This is the first report of artificial pinning centers being successfully incorporated into $REBa_2Cu_3O_{7-x}$ (REBCO, $RE = Y, Gd, Dy \ldots$) via EB-PVD. The samples were grown on Hastelloy tapes coated with a MgO buffer layer deposited by inclined substrate deposition. The J_c of the samples was characterized at 77 K, 1 T and at 30 K, 3 T. An increase in J_c (30 K, 3 T) upon Hf addition has been observed in the whole angular range α. The level of Hf addition was found to heavily influence the kind of nanoprecipitate formed, with low levels of Hf causing a reduction in the anisotropy of J_c (77 K, 1 T) and higher levels of Hf resulting in the formation of nanoprecipitates elongated parallel to the GdBCO ab-plane, causing an increase in the anisotropy of J_c (77 K, 1 T). The largest J_c (77 K, sf) measured was 0.63 MA/cm^{-2}.**

***Index Terms*—BHO, coated conductor, EB-PVD, flux pinning, GdBCO.**

I. Introduction

HIGH-TEMPERATURE superconductors (HTS) based on $RE\text{Ba}_2\text{Cu}_3\text{O}_{7-x}$ (REBCO, $RE = \text{Y, Gd, Dy} \ldots$) are now viable for use in superconducting rotating machines [1]. $GdBa_2Cu_3O_{7-x}$ (GdBCO) is one such HTS material which, when deposited as a film on a flexible metallic tape, constitutes a second generation (2G) coated conductor (CC) [2]. Hastelloy C-276 is a favored CC substrate as it is non-magnetic, has large yield strength and a strong corrosion-resistance [3], [4]. The aim of the CC industry is to produce large quantities of HTS tape at low cost. One method of keeping costs low is using fewer fabrication steps. Inclined substrate deposition (ISD) is an excellent, scalable technique for creating a biaxially textured MgO layer on the polycrystalline Hastelloy [5]–[7]. This provides a template upon which a biaxially textured GdBCO film can grow heteroepitaxially whilst eliminating the requirement for numerous additional buffer layers. Also key to quality CC production are the deposition techniques of the various layers. Numerous methods of HTS deposition exist in industry, including pulsed laser deposition (PLD) [8] and metal-organic chemical vapor deposition (MOCVD) [9]. The electron beam physical vapor deposition (EB-PVD) method, however, is one of the most attractive industrial methods for deposition of HTS films [10]. An improvement in critical current density (J_c) under the conditions required by superconducting motors and generators (30 K, 3 T) is still desired before HTS CCs can be successfully implemented. This goal has been addressed by the introduction of artificial pinning centers of $\text{Ba}MO_3$ ($\text{B}MO, M = \text{Hf, Zr, Sn} \ldots$) to the HTS matrix in order to pin flux lines [11]–[13]. $BaHfO_3$ (BHO) has been demonstrated as a good candidate for improving pinning in GdBCO coated conductors through the formation of nano-sized BHO inclusions [14].

In order to improve J_c at 30 K, 3 T of coated conductors fabricated on ISD via EB-PVD, it is crucial to improve the understanding of the mechanisms by which certain pinning centers can be formed with this deposition method and on this buffer layer. Only once an understanding is made of which possible pinning landscapes exist can the multitude of deposition conditions be optimized and the most effective pinning be achieved.

Here we show the influence of Hf content and deposition temperature (T_{dep}) on J_c at 77 K, 1 T and 30 K, 3 T and on the transition temperature (T_c) of GdBCO films grown via EB-PVD.

II. Experimental Details

GdBCO coated conductors were prepared via EB-PVD of a GdBCO granulate (grain size < 0.5 mm) onto a Hastelloy/ MgO-ISD/MgO cap layer architecture as published previously [10]. Oxygen annealing and deposition of a silver contact layer was carried out *ex situ*. During the deposition the sample surface temperature was monitored via pyrometer and could be kept constant to within 7 °C throughout the deposition. The rate was measured via quartz crystal microbalance. For Hf-doped GdBCO samples, the GdBCO granulate was mixed with HfO_2

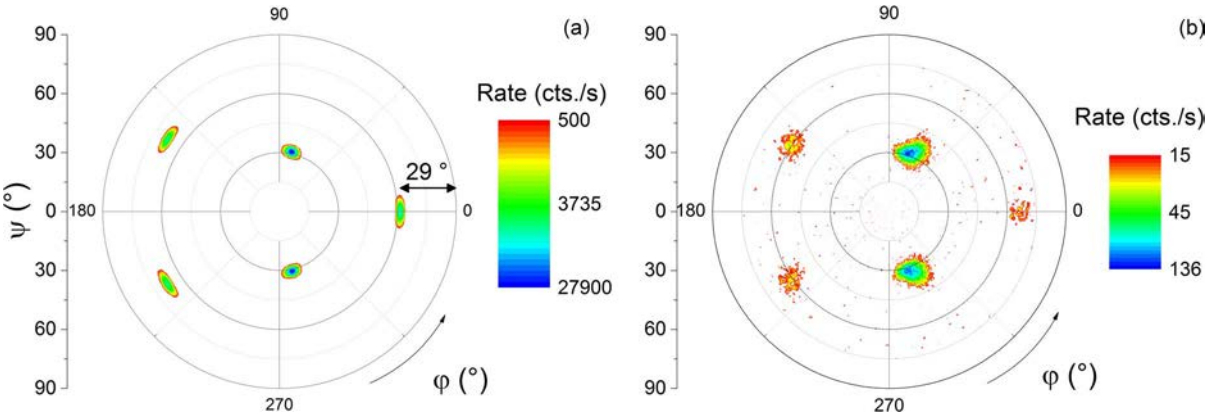

Fig. 1. Pole figures of (a) an undoped GdBCO sample deposited at 662 °C showing the GdBCO (103) plane and (b) a 11.8 mol.% BHO-doped sample deposited at 710 °C showing the BHO (110) plane.

powder. The HfO_2 powder was of small enough grain size to coat the larger GdBCO grains (roughly 300 times smaller than that of GdBCO). Mixing was carried out by combining the HfO_2 powder and GdBCO granulate in a mixing vessel and shaking until the mixture was of uniform composition. All GdBCO films deposited were 1 μm thick.

Sample stoichiometry was measured by inductively coupled plasma mass spectroscopy (ICP-MS). Sample thickness and surface morphology were analyzed via scanning electron microscopy (SEM) using a *Hitachi SU8000*. Thickness measurements were made on sample cross sections prepared using a *Hitachi E-3500* ion milling system.

X-ray diffraction pole figures of the GdBCO (103) and BHO (110) diffraction peaks were made via two-axis measurements (out-of-plane $\psi = 0° - 80°$, in-plane $\varphi = 0° - 360°$) using a *Philips X'Pert X-Ray Diffractometer* with Cu-K_α radiation.

For electrical characterization, bridges of 800 μm in length and 20 μm in width were prepared parallel to the rolling tape direction by laser cutting [15]. T_c and J_c were measured resistively in a four-point geometry on the bridges using a *Quantum Design Physical Property Measurement System* (PPMS) equipped with a 9 T magnet. T_c was defined as the temperature at which the superconductor reaches zero resistivity. J_c was determined from current density vs. electric field curves using the 1 μV/cm criterion. J_c was measured at 77 K, self-field (sf) and as a function of the angle of the applied magnetic field with the tape surface normal (α) in the maximum Lorentz force configuration at 77 K, 1 T and 30 K, 3 T.

High-angle annular dark-field (HAADF) scanning transmission electron microscopy (STEM) was carried out using a *FEI Titan^3 G2 60-300* (Fraunhofer IWMS, Halle/Saale, Germany).

III. Results and Discussion

A. X-Ray Diffraction

The epitaxial growth of GdBCO on MgO is revealed through the GdBCO (103) pole figure $(2\theta = 32.5°)$ in Fig. 1(a). The pole figure depicts the four-fold symmetry of the GdBCO (103) plane. The tilt of the crystallographic structure of 29° with respect to the sample surface can be seen from the displacement of the GdBCO (110) reflection from $\psi = 90°$. Fig. 1(b) shows the BHO (110) pole figure of a 11.8 mol.% Hf-doped sample taken at $2\theta = 29.8°$. The tilt angle for this sample is 24°. This difference in tilt angle between the two pole figures is within the limits of ISD tilt variation across different ISD samples. The BHO (110) plane is clearly aligned parallel to the GdBCO (103) plane, indicating a biaxially c-axis textured relationship.

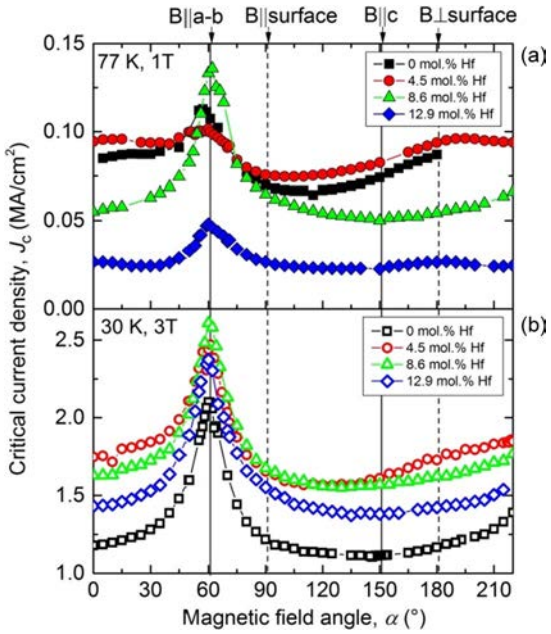

Fig. 2. J_c as a function of the angle of the magnetic field with the tape surface normal at (a) 77 K, 1 T and (b) 30 K, 3 T for four GdBCO samples with different BHO contents deposited at (660 ± 7)°C.

B. In-Field Critical Current Density

Fig. 2(a) shows J_c as a function of α for samples with a Hf content of 0 mol.%, 4.5 mol.%, 8.6 mol.% and 12.9 mol. % deposited at (660 ± 7) °C. At 77 K, 1 T, addition of 4.5 mol.% Hf shows a small increase in the minimum J_c accompanied by a decrease in the peak at 61°, which is associated with pinning at extended, correlated defects parallel to the ab-plane, such as stacking faults [16] and precipitates (see below). The

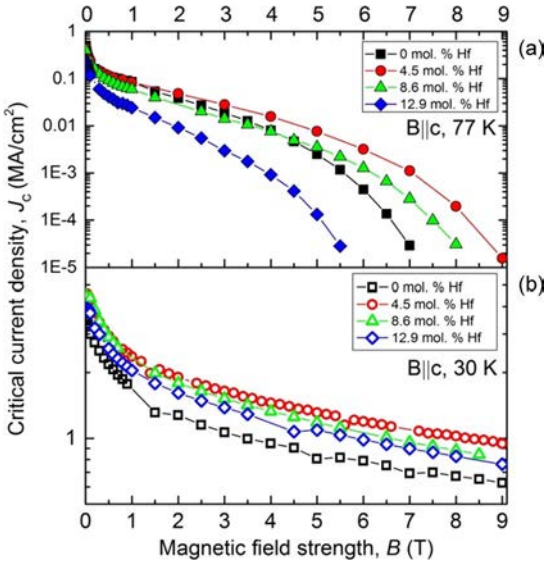

Fig. 3. J_c as a function of magnetic field strength with $B\|c$ for four GdBCO samples with different BHO contents deposited at (660 ± 7) °C.

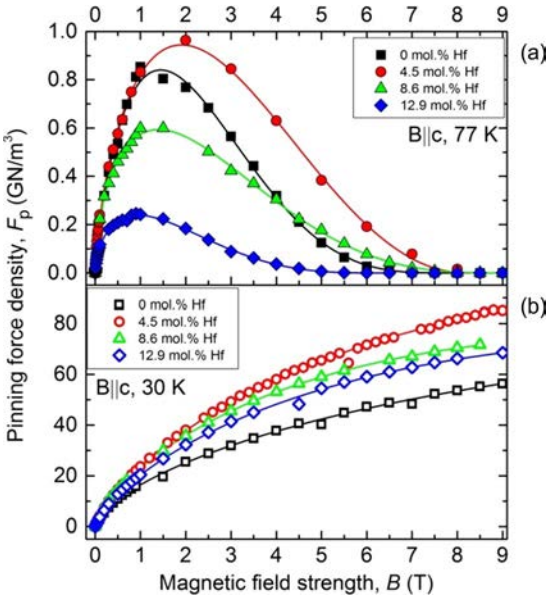

Fig. 4. F_p as a function of magnetic field strength with $B\|c$ for four GdBCO samples with different BHO contents deposited at (660 ± 7)°C.

broad peak centered close to the tape normal (180°–195°) can be attributed to pinning at grain boundaries, which are aligned, on average, in the same direction. This disappears at high fields and low temperatures [16]. Samples prepared with higher Hf content show a decrease in J_c over all α compared to the undoped sample. The same samples are measured at 30 K, 3 T in Fig. 2(b). These all display an increase in J_c, compared to the undoped sample, in the whole angular range, with the largest J_c observed for 4.5 mol.% Hf. The grain boundary peak decreases for all but the 4.5 mol.% Hf sample, for which a small, broad region remains around the surface normal. Interesting is the absence of a peak parallel to the c-axis, which normally occurs in GdBCO coated conductor samples with added Hf deposited via vapor phase epitaxy [17]. This is addressed in section C, below.

The magnetic field dependence of J_c for the same samples, measured at 77 K with $B\|c$, is shown in Fig. 3(a). At 77 K an increase in J_c is observed above 1 T for 4.5 mol.% Hf addition and above 4 T for 8.6 mol.% Hf. J_c is decreased under all measured B up to 9 T for the 12.9 mol.% Hf sample. Fig. 3(b) shows the same relationship measured at 30 K, in which an increase J_c is clearly visible for all Hf additions, with 4.5 mol.% Hf resulting in the largest J_c for all measured fields up to 9 T.

In Fig. 4(a) the pinning force density $(F_p = J_c \times B)$ at 77 K is displayed as a function of B. The maximum F_p for the undoped sample is 0.85 GN/m^3 at 1 T. The 4.5 mol.% Hf added sample shows a maximum F_p of 0.96 GN/m^3 at 2 T. The 8.6 mol.% Hf added sample shows F_p values larger than the undoped sample only above 4 T. Fig. 4(b) shows the $F_p - B$ relationship at 30 K. Again all Hf-added samples show a larger F_p than the undoped sample. Up to 0.7 T the 4.5 mol.% and 8.6 mol.% Hf containing samples show nearly the same dependence on B. From 0.7 T to 9 T the 4.5 mol.% Hf sample shows the highest F_p, with 85 GN/m^3 at 8.8 T the largest value measured. The maximum of the curve was not reached.

In order to achieve high J_c (30 K, 3 T) not only is the optimum Hf content important but also the optimum T_{dep}. Various T_{dep} at various Hf contents were therefore investigated. The sample deposited with 8.6 mol.% Hf at 675°C displayed the largest overall J_c, with J_c (77 K, self-field) $= 0.63$ MAcm^{-2} and a minimum J_c (30 K, 3 T) over all α of 2.33 MAcm^{-2}. The undoped sample showed J_c (77 K, self-field) $= 0.50$ MAcm^{-2}. These values are low compared with previously published results, where a J_c (77 K, self-field) of 2.5 MAcm^{-2} was achieved for undoped samples [10]. This is due to unoptimized film stoichiometry. The undoped sample in this paper was found to have a film stoichiometry with 2.0% Gd excess and 1.7 % Cu deficiency compared to the known optimum. Preliminary stoichiometry optimization depositions have already yielded samples with J_c (77, self-field) of 1.11 MA/cm^2 for 4.3 mol.% Hf addition.

Fig. 5(a) and (b) shows the minimum J_c $(J_{c,\min})$ measured at 77 K, 1 T and at 30 K, 3 T, over all α plotted as a function of Hf content and T_{dep}. The largest J_c is achieved for 8.6 mol.% Hf deposited at 675 °C. In Fig. 5(c) T_c (defined as the temperature at which the superconductor reaches zero resistivity) is depicted as a function of Hf content and T_{dep}. The plot follows a similar trend as in Fig. 5(a), indicating that T_c suppression has a heavy influence on $J_{c,\min}$ (77 K, 1 T). The similarity between Fig. 5(b) and (c) is far less as T_c suppression has a much lesser influence on $J_{c,\min}$ (30 K, 3 T). It is known that a reduction in T_c accompanied by the addition of BMO is a result of strain-induced crystalline defects [18], [19]. Increasing T_{dep} clearly negates this formation of additional defects, as can be seen by the lower $J_{c,\min}$ (30 K, 3 T) in Fig. 5(b) and the higher T_c in Fig. 5(c) at increased T_{dep}.

C. Transmission Electron Microscopy

Fig. 6(a)–(d) shows a HAADF STEM image along with the corresponding EDX maps of the 12.9 mol.% Hf sample deposited at 667 °C. The EDX maps clearly show Hf- and Gd-containing precipitates 2.8 nm–17.0 nm in width and up to

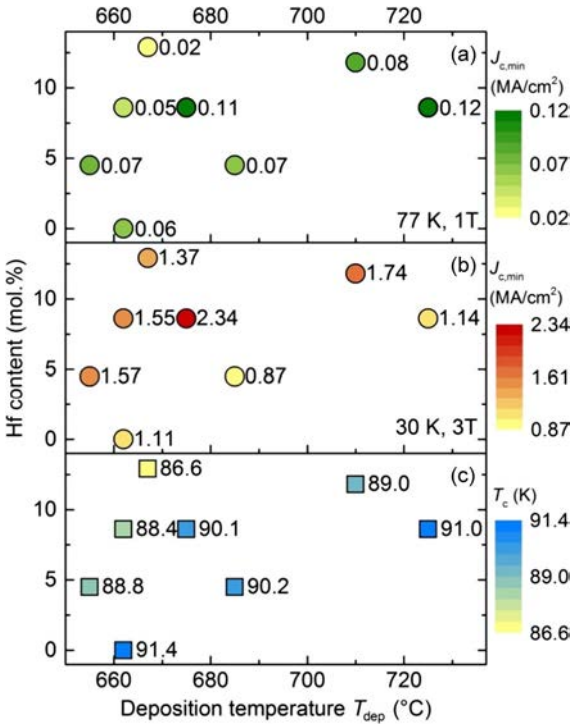

Fig. 5. (a) Minimum J_c at 77 K, 1 T, (b) minimum J_c at 30 K, 3 T, and (c) zero resistivity T_c plotted versus Hf content and deposition temperature T_{dep}.

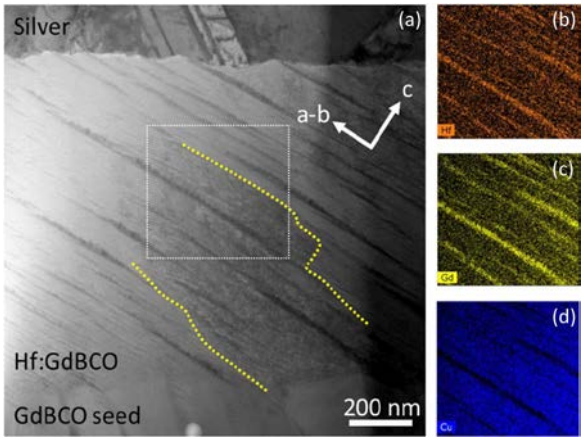

Fig. 6. (a) HAADF STEM micrograph of the film cross section perpendicular to the tape direction. The white arrows indicate the GdBCO c-axis and ab-plane directions, and the dashed yellow lines mark grain boundaries. The white square indicates the area taken for the colored EDX maps showing (b) Hf, (c) Gd, and (d) Cu. The scale bar is valid for all four images.

716 nm in length aligned parallel to the ab-plane. Grain boundaries, marked in yellow, are visible and aligned much closer to the ab-plane than previously published for non Hf-added samples grown on ISD via EB-PVD [16].

The addition of Hf thus does not result in the growth of nanorods aligned parallel to the GdBCO c-axis as shown for other samples deposited via vapor phase epitaxy. This explains the absence of a peak around $B\|c$ in Fig. 2. Rather, addition of Hf in larger quantities results in one or more nano-sized phases, including BHO, aligned parallel to the GdBCO ab-plane. This also influences the alignment of the grain boundaries, with the precipitates forcing grain boundaries, which would otherwise be aligned close to the surface normal, to align parallel to the GdBCO ab-plane. Thus the grain boundary peak in Fig. 2(a) disappears.

For addition of smaller quantities of Hf (4.5 mol.%), an increase in J_c at 30 K, 3 T is observed across all α and B. The grain boundary peak at 77 K, 1 T remains close to the surface normal indicating in this case far fewer nanoprecipitates parallel to the ab-plane. This increase in J_c would therefore be explained by the presence of pinning centers randomly distributed throughout the film.

It is likely that the absence of c-axis aligned nanorods is due either to the growth of the GdBCO in a tilted geometry on the ISD substrate or due to the EB-PVD process; however from present results the two effects cannot yet be differentiated.

IV. Conclusion

We have found that BHO pinning centers can be easily incorporated into GdBCO films prepared via EB-PVD by simply mixing HfO_2 powder with the GdBCO granulate before evaporation. The addition of Hf in smaller quantities (4.5 mol.%) reduces the anisotropy of J_c at 77 K, 1 T while addition of Hf in larger quantities ($>$ 8 mol.%) increases the anisotropy of J_c at 77 K, 1 T. The addition of 4.5 mol.% Hf was found to result in the highest increase in J_c at 30 K, 3 T without greatly affecting grain boundary alignment, which could be explained through introduction of randomly distributed pinning centers. An increase in deposition temperature in turn reduces the effective pinning.

Acknowledgment

The authors thank R. Nast and J. Handke for technical assistance and W. Prusseit and P. Pahlke for helpful discussion.

References

[1] G. Snitchler, B. Gamble, C. King, and P. Winn, "10 MW class superconductor wind turbine generators," *IEEE Trans. Appl. Supercond.*, vol. 21, no. 3, pp. 1089–1092, Jun. 2011.

[2] S. Kang *et al.*, "High-performance high-T_c superconducting wires," *Science*, vol. 311, no. 5769, pp. 1911–1914, Mar. 2006.

[3] J. Lu, E. S. Choi, and H. D. Zhou, "Physical properties of Hastelloy® C-276™ at cryogenic temperatures," *J. Appl. Phys.*, vol. 103, pp. 1911–1914, Mar. 2008.

[4] Haynes International Inc., Brochure H-2002D, [Accessed: March 1, 2016]. [Online]. Available: http://www.haynesintl.com/pdf/h2002.pdf.

[5] M. Bauer, R. Metzger, R. Semerad, P. Berberich, and H. Kinder, "Inclined substrate deposition by evaporation of magnesium oxide for coated conductors," in *Proc. Mater. Res. Soc. Symp.*, 2000, vol. 585, pp. 35–44.

[6] M. Bauer, R. Semerad, and H. Kinder, "YBCO films on metal substrates with biaxially aligned MgO buffer layers," *IEEE Trans. Appl. Supercond.*, vol. 9, no. 2, pp. 1502–1505, Jun. 1999.

[7] W. Prusseit *et al.*, "Long length coated conductor fabrication by inclined substrate deposition and evaporation," *J. Phys. Conf. Ser.*, vol. 43, pp. 215–218, 2006.

[8] K. Kakimoto *et al.*, "Long RE123 coated conductors with high critical current over 500 A/cm by IBAD/PLD technique," *Phys. C, Supercond.*, vol. 471, no. 21/22, pp. 929–931, Nov. 2011.

[9] V. Selvamanickam *et al.*, "High performance 2G wires: From R&D to pilot-scale manufacturing," *IEEE Trans. Appl. Supercond.*, vol. 19, no. 3, pp. 3225–3230, Jun. 2009.

[10] W. Prusseit *et al.*, "ISD process development for coated conductors," *Phys. C, Supercond. Appl.*, vol. 426–431, pp. 866–871, Jul. 2005.

[11] J. L. MacManus-Driscoll *et al.*, "Strongly enhanced current densities in superconducting coated conductors of $YBa_2Cu_3O_{7-x}$ $+BaZrO_3$," *Nature Mater.*, vol. 3, no. 7, pp. 439–443, Jul. 2004.

[12] M. Miura *et al.*, "The effects of density and size of $BaMO_3$ ($M = Zr, Nb, Sn$) nanoparticles on the vortex glassy and liquid phase in (Y,Gd)$Ba_2Cu_3O_y$ coated conductors," *Supercond. Sci. Technol.*, vol. 26, 2013, Art. no. 035008.

[13] M. Sieger *et al.*, "$BaHfO_3$-doped thick $YBa_2Cu_3O_{7-\delta}$ films on highly alloyed textured Ni–W tapes," *IEEE Trans. Appl. Supercond.*, vol. 25, no. 3, Jun. 2015, Art. no. 6602604.

[14] H. Tobita *et al.*, "Fabrication of $BaHfO_3$ doped $Gd_1Ba_2Cu_3O_{7-\delta}$ coated conductors with the high I_c of 85 A/cm-w under 3 T at liquid nitrogen temperature (77 K)," *Supercond. Sci. Technol.*, vol. 25, May 2012, Art. no. 062002.

[15] R. Nast *et al.*, "Influence of laser striations on the properties of coated conductors," *J. Phys., Conf. Ser.*, vol. 507, no. 2, 2014, Art. no. 022023.

[16] M. Lao *et al.*, "Critical current anisotropy of GdBCO tapes grown on ISD-MgO buffered substrate," *Supercond. Sci. Technol.*, vol. 28, Oct. 2015, Art. no. 124002.

[17] D. Yokoe *et al.*, "Transmission electron microscopy study of $GdBa_2Cu_3O_{7-x}$ containing nano-sized $BaMO_3$ (M: Hf, Zr, Sn) rods fabricated by pulsed laser deposition," *J. Mater. Sci.*, vol. 48, pp. 125–131, Sep. 2012.

[18] M. Peurla *et al.*, "Optimization of the $BaZrO_3$ concentration in YBCO films prepared by pulsed laser deposition," *Supercond. Sci. Technol.*, vol. 19, pp. 767–771, Jun. 2006.

[19] V. Selvamanickam *et al.*, "Enhanced critical currents in (Gd,Y)$Ba_2Cu_3O_x$ superconducting tapes with high levels of Zr addition," *Supercond. Sci. Technol.*, vol. 26, Jan. 2013, Art. no. 035006.